



HAL
open science

Post-Implantation Annealing of Aluminium in 6H-SiC

Laurent Ottaviani, Dominique Planson, Marie-Laure Locatelli, Jean-Pierre Chante, B. Canut, S. Ramos

► **To cite this version:**

Laurent Ottaviani, Dominique Planson, Marie-Laure Locatelli, Jean-Pierre Chante, B. Canut, et al.. Post-Implantation Annealing of Aluminium in 6H-SiC. Materials Science Forum, 1998, 264-268, pp.709-712. 10.4028/www.scientific.net/MSF.264-268.709 . hal-02281029

HAL Id: hal-02281029

<https://hal.science/hal-02281029>

Submitted on 7 Sep 2019

HAL is a multi-disciplinary open access archive for the deposit and dissemination of scientific research documents, whether they are published or not. The documents may come from teaching and research institutions in France or abroad, or from public or private research centers.

L'archive ouverte pluridisciplinaire **HAL**, est destinée au dépôt et à la diffusion de documents scientifiques de niveau recherche, publiés ou non, émanant des établissements d'enseignement et de recherche français ou étrangers, des laboratoires publics ou privés.

Post-Implantation Annealing of Aluminum in 6H-SiC

L. Ottaviani¹, D. Planson¹, M.L. Locatelli¹, J.P. Chante¹,
B. Canut² and S. Ramos²

¹ CEGELY (UPRES-A CNRS n°5005), Bât. 401, INSA de Lyon,
20, av. Einstein, F-69621 Villeurbanne Cedex, France

² Département de Physique de Matériaux (UMR CNRS n°5586), Université C. Bernard LYON I,
43, Boulevard du 11 Novembre 1918, F-69622 Villeurbanne Cedex, France

Keywords: Ion Implantation, Annealing Atmosphere, Surface Stoichiometry, RBS/Channeling

ABSTRACT Two double aluminum implantations at room temperature were performed in two p-type epitaxial 6H-SiC wafers, with a maximum energy of 320 keV and a total fluence of $1.6 \cdot 10^{15} \text{ cm}^{-2}$. The two samples were then annealed in a rf furnace at 1700°C during 30 minutes, one with a SiC plate inside the reactor and the other without. RBS/C spectra were recorded on the implanted faces of each sample, before and after annealing. We observed that the implantation induced the amorphization of the material, and that the damaged layer of the sample annealed with the SiC plate was less extended in depth than the other. Moreover, the solid phase epitaxy appears to occur at two interfaces in the first case, that is the recrystallization arises from the volume and from the surface. The explanation of this phenomenon could be outlined from the XPS results, which show a better surface stoichiometry when the SiC plate is inside the reactor. This plate gives therefore interesting effects and improvements on the crystallinity and stoichiometry of the annealed sample.

1. INTRODUCTION

Ion implantation is a necessary process for the elaboration of SiC electronic components, to create localised p-n junctions in the material. Thermal annealing is then required for two main reasons : it is necessary to recrystallize the matrix which can be, if the dose is sufficiently high, totally amorphized. Next the incorporated atoms must diffuse to substitutional sites in order to be electrically active. So, the technical characteristics of the annealing must be determined precisely to optimize the crystal regeneration.

In order to investigate this point, we performed double aluminum implantations at room temperature in two p-type epitaxial SiC layers, issued from the same CREE wafer. The tilt angle was chosen to minimize the channeling effect (7° off the target normal). The energies and associated fluences were : 320 keV with $1 \cdot 10^{15} \text{ cm}^{-2}$, and 160 keV with $6 \cdot 10^{14} \text{ cm}^{-2}$. According to TRIM 94 code calculations [1], the projected ranges are 177 nm for 160 keV, and 356 nm for 320 keV. The total fluence is $1.6 \cdot 10^{15} \text{ cm}^{-2}$, i. e. above the critical threshold for amorphization which is about $8 \cdot 10^{14} \text{ cm}^{-2}$ for Al in 6H-SiC [2].

The annealings were carried out in nitrogen atmosphere, in a furnace heated by a radiofrequency generator. The quartz reactor contained a glassycarbon tube, a graphite susceptor and a graphite cover. We studied the influence of the presence inside the reactor of a SiC plate, set at the top of the graphite cover (see Fig. 1). This plate was first introduced in order to limit the sample energy losses by emissivity, and to shield the upper silicon gasket of the furnace. The two samples were annealed at 1700°C during 30 minutes : the sample A without the plate, and B with the plate. We notice that each one was annealed with the implanted side placed on the susceptor, since (SiC + C) is a more stabilized thermodynamical system than SiC, and improves so the process reproducibility.

Both samples were characterized before and after annealing with X-Ray Photoelectron Spectroscopy (XPS) to analyse the surface stoichiometry, and with Rutherford Backscattering Spectrometry in Channeling geometry (RBS/C) to measure the lattice disorder. The technical characteristics of these analyses will be found in Ref. [3], which relates the results of the RBS/C, XPS and optical absorption measurements on the sample A before and after annealing.

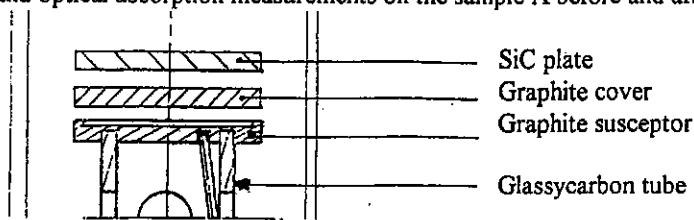


Fig.1 *Reactor configuration*

2. EVOLUTION OF THE SURFACE STOICHIOMETRY AND CHEMICAL BONDS

The SiC plate was thought to prevent partial Si sublimation from the SiC sample, which otherwise frequently occurs at 1400°C leaving a C-rich disordered surface layer [4]. In order to study the evolution of surface stoichiometry and the chemical bonds nature, XPS spectra were undertaken on the unimplanted sides of the samples, after Ar⁺ sputtering at low pressure.

Si_{2p}

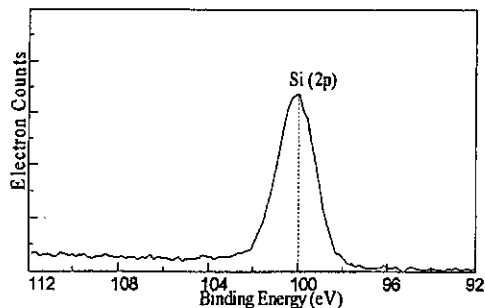


Fig.2 *Sample B at 10 nm : Si_{2p} core line*

The Si_{2p} spectrum displayed in Fig.2 was recorded on the post-annealed sample B at a depth of 10 nm. A well resolved peak centered at 100.04 eV binding energy is clearly observed, and ascribed to Si-C bonds.

Ref. [3] presents the XPS spectra recorded on the post-annealed sample A at the same depth. The Si_{2p} peak is then centered at 101.20 eV. The energy shift is due to the SiO_xC_y bonds appeared after the annealing without SiC plate.

C_{1s}

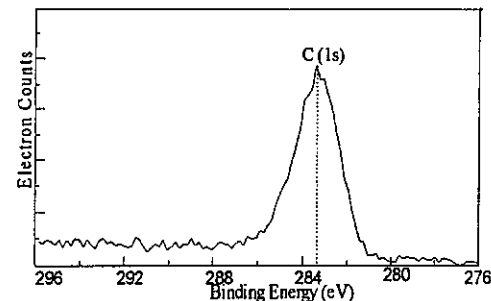


Fig.3 *Sample B at 10 nm : C_{1s} core line*

Fig.3 presents the C_{1s} spectrum on the post-annealed sample B at 10 nm. The peak is centered at 283.2 eV, which is the classical value for C-Si bonds.

The same core line of the post-annealed sample A (see Ref.[3]) is shifted and located at 284.6 eV. This latter binding energy may be attributed to the C-C and/or C-H bonds. The surface graphitization is then evident.

XPS analysis gives also the atomic ratios of the different elements present in the material, and so allows the calculation of surface stoichiometry. The obtained values of [Si/C] at the depth of 10 nm are : 0.40 with sample A, and 0.84 with the sample B. The SiC plate gives then a better surface stoichiometry, that is the sublimation of Si is thermodynamically decreased because of the highest Si partial pressure in the furnace reactor. Moreover, the SiC plate favors Si-C bonds in the

of 10 nm are : 0.40 with sample A, and 0.84 with the sample B. The SiC plate gives then a better surface stoichiometry, that is the sublimation of Si is thermodynamically decreased because of the highest Si partial pressure in the furnace reactor. Moreover, the SiC plate favors Si-C bonds in the surface material : we notice that there are less C-C, C-H and SiO_xC_y bonds, and so less surface graphitization.

3. EVOLUTION OF THE DAMAGED LAYER

2 MeV $^4\text{He}^+$ RBS/C results on the evolution of irradiation damage in both samples, before and after the annealing, are shown in Fig.4.

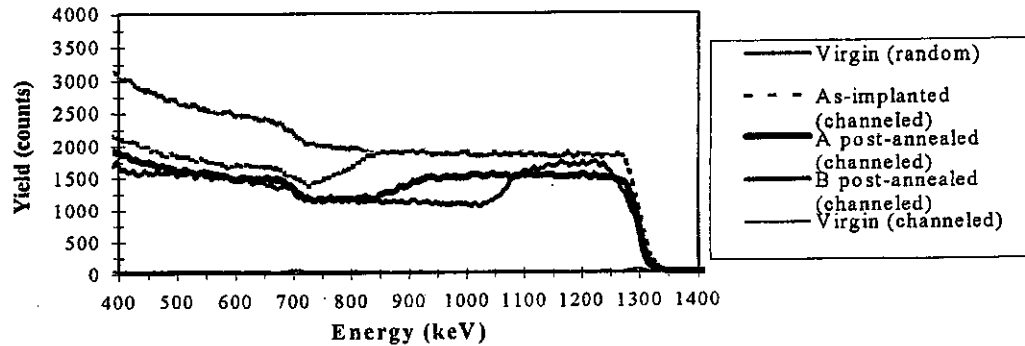


Fig. 4 RBS/C spectra of the virgin, as-implanted and post-annealed samples

We notice that the aligned spectrum actually coincides with the random one (from the virgin sample), from the high energy edge of Si (1300 keV) to a minimum energy of about 850 keV. Since the total dose exceeded the threshold for amorphization, we can conclude that this implantation induced a totally amorphized layer. We have assumed during all this work that SiC density remained constant during ion implantation, with the value of 3.2 g.cm^{-3} . This allows us to determine an amorphized layer depth value of about $0.40 \mu\text{m}$ from the surface.

TRIM calculations give the Si vacancies distribution versus depth (see Fig.5). This curve is drawn using the critical deposited damage energy for amorphization as $2 \cdot 10^{21} \text{ keV/cm}^3$ [5], and the calculations are carried out with the Kinchin-Pease local model [1].

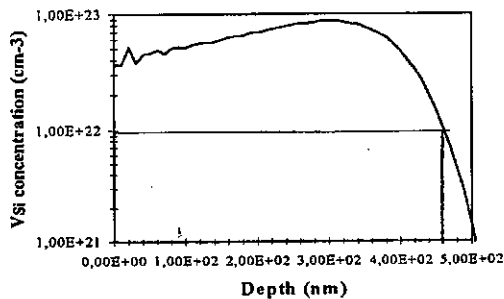


Fig.5 Si vacancies vs depth (TRIM Code)

Spitznagel *et al.* [5] explain that the amorphization criterion corresponds to a displacement of approximately 10% of the lattice for room temperature implantation. Considering the SiC atomic density ($9.66 \cdot 10^{22} \text{ cm}^{-3}$), Fig.5 reports an amorphized layer thickness of $\sim 0.46 \mu\text{m}$ with this criterion. The depth determined with the RBS/C analysis ($0.40 \mu\text{m}$) must then be underestimated, because the amorphous SiC density is probably reduced to about 2.9 g.cm^{-3} [6].

Sample A

After the annealing (without SiC plate), we observe a partial recrystallization from the volume which induced a damaged layer thickness of about $0.33 \mu\text{m}$. A mean dechanneling yield of 80% indicates the presence of residual defects in the material. Chechenin *et al.* [2] explain this disorder region by the presence of very dense extended defects with a high dechanneling cross section. They also demonstrate that the Al atoms move into regions with high defect

concentration, which have two maxima : one in the surface region, and the other in depth. In our case, the defects near the surface appeared during the annealing are probably the silicon vacancies issued from the thermal sublimation of Si.

The solid-phase epitaxy in volume consists in the rearrangement of the 'end-of-range' defects, so-called Type II defects by Fair *et al.* [7], and which take place only when an amorphous layer is formed. Their location is below the amorphous/crystalline interface, and they mostly are produced by the coalescence of point defects (especially interstitials) into small diameter dislocation loops during the annealing.

Sample B

Three phenomena have to be noticed : (1) the damaged layer is approximately half thinner than the sample A, the depth of the amorphous/crystalline interface in volume is about **0.16 μm** ; (2) the mean dechanneling yield of the damaged layer is 90%; (3) there are two interfaces of solid-phase epitaxy (in volume and at surface).

XPS spectra indicated the better surface crystallinity after annealing with the presence of the SiC plate, in terms of stoichiometry and chemical bonds. Aluminum atoms might consequently less diffuse towards the surface, because of the reduced density of trapping sites and lattice vacancies in this zone. This could then produce a more active recombination of Al atoms with the volume defects induced by the implantation, because there is only one region with high defect concentration. And this can therefore explain the higher regrowth rate of the amorphous/crystalline interface at volume (almost twice of sample A).

Fair *et al.* [7] introduce in this case the Type IV damages, which are dislocation loops between the two solid-phase epitaxy interfaces, and due to mismatch between the crystal layers. This explains the high dechanneling yield of the damaged layer, but these defects have been shown to be less stable in silicon than Type II defects, and so disappear rapidly with anneal duration.

4. CONCLUSION

The presence of a SiC plate in a furnace reactor during a post-aluminum implantation annealing improves the surface crystallinity of the material, and favors so the recrystallization process in increasing its velocity. Further investigations are in progress to verify the electrical activation improvement of the Al atoms, and to determine the variation of these phenomena with the annealing duration.

References

- [1] J.F. Ziegler, J.P. Biersack, and U. Littmark, *The Stopping and Range Ions in Solids* (Pergamon, New York, 1985), Vol. I.
- [2] N.G. Chechenin, K.K. Bourdelle, A.V. Suvorov, and A.X. Kastilio-Vitloch, *Nucl. Instr. And Meth. B65* (1992), p. 341.
- [3] B. Canut, S. Ramos, J.A. Roger, J.P. Chante, M.L. Locatelli, and D. Planson, *Mater. Sci. Eng. B46* (1997), p. 267.
- [4] M. Ghezzi, D.M. Brown, E. Downey, J. Kretschmer, W. Hennessy, D.L. Polla, and H. Bakhru, *IEEE Electron. Device Lett.* 13 (1992), p. 639.
- [5] J.A. Spitznagel, S. Wood, W.J. Choyke, N.J. Doyle, J. Bradshaw, and S.G. Fishman, *Nucl. Instr. And Meth. B16* (1986), p. 237.
- [6] V. Heera, J. Stoemenos, R. Kögler, and W. Skorupa, *J. Appl. Phys.* 77 (1995), p. 2999.
- [7] R. Fair, K.S. Jones and G.A. Rozgony, *Rapid thermal processing : science and technology* (Academic Press, San Diego, 1993).